DALTON
FULL PAPER

Synthesis of molybdenum arene complexes containing amide-derived heterodifunctional P,O ligands

Neale G. Jones,[a] Malcolm L. H. Green,*[a] Ino Vei,[a] Andrew Cowley,[a] Xavier Morise *[b] and Pierre Braunstein *[b]

[a] *Inorganic Chemistry Laboratory, University of Oxford, South Parks Road, Oxford, UK OX1 3QR. E-mail: Malcolm.Green@chemistry.oxford.ac.uk*
[b] *Université Louis Pasteur (UMR 7513 CNRS), 4 rue Blaise Pascal, F-67070 Strasbourg, France. E-mail: morise@chimie.u-strasbg.fr; braunst@chimie.u-strasbg.fr*

Received 5th July 2001, Accepted 2nd January 2002
First published as an Advance Article on the web 26th February 2002

The reactions of the amide-derived ligands $Ph_2PN(R)C(O)CH_3$ (R = H, CH_3) with the molybdenum arene complexes $[Mo(\eta^3\text{-}C_3H_5)(\mu\text{-}Cl)(\eta^6\text{-}C_6H_5R)]_2$ (R = H, CH_3) have been investigated. A series of complexes in which the functional ligand displays η^1-phosphine, η^2-acetamidophosphine and η^2-phosphinoiminolate coordination have been synthesised and characterised. The crystal structures of the cationic compounds $[Mo(\eta^3\text{-}C_3H_5)(\eta^6\text{-}C_6H_6)\text{-}\{Ph_2PN(R)C(O)CH_3\text{-}\kappa^2P,O\}][PF_6]$ (R = H, CH_3) have been determined. The first example of a structurally characterised phosphinoiminolate complex $[Mo(\eta^3\text{-}C_3H_5)(\eta^6\text{-}C_6H_6)\{Ph_2PN{=}C({-}O)CH_3\text{-}\kappa^2P,O\}]$ is also reported.

Introduction

Heterodifunctional chelating ligands which combine a soft phosphine donor with a hard oxygen functionality are well known and the chemistry of their various transition metal complexes widely studied, in particular with respect to their role in homogeneous catalysis and their potentially hemilabile behaviour.[1–3]

In recent times, heterodifunctional ligands possessing P–N bonds have emerged as an interesting class of ligands. For example, comparisons between the reactivity of the related ligands, bis(diphenylphosphino)methane (dppm) and bis(diphenylphosphino)amine (dppa) have been reported.[4–7] The reactions of a P,N mixed donor ligand $Ph_2PN(H)Py$ with various late transition metal complexes have also been described.[8,9]

The amide-derived ligands, $Ph_2PN(R)C(O)CH_3$ (R = H, CH_3)[10] and $Ph_2PN(H)C(O)R$ (R = Ph, NH_2, 3-pyridyl)[11,12] represent new difunctional P,O ligands for late transition metal complexes. The acetamide-derived P,O donor ligands have been observed to be more effective chelating ligands than $Ph_2PCH_2C(O)Ph$. These have also been found to act as efficient stabilising ligands for cationic Pd complexes and have allowed the direct observation and characterisation of intermediates in the sequential insertion of CO, ethene, CO and ethene or methylacrylate into a Pd-methyl bond.[13]

The early transition metal chemistry of the phosphine ligands containing a carbonyl group, such as a ketone, ester or amide function, is relatively underdeveloped. However, half-sandwich molybdenum complexes of the amidophosphine $Ph_2PCH_2C(O)NPh_2$[14] and the keto-functionalised N-pyrrolylphosphine $Ph_2PNC_4H_3\{C(O)CH_3\}$-2[15] have been recently reported. Here we describe the chemistry of heterodifunctional acetamido P,O donor ligands with molybdenum(II) arene complexes.

Results and discussion

The reaction between $[Mo(\eta^3\text{-}C_3H_5)(\mu\text{-}Cl)(\eta^6\text{-}C_6H_5CH_3)]_2$ and *N*-(diphenylphosphino)acetamide L^1 in toluene resulted in cleavage of the chloro-bridged dimer to afford the phosphine adduct $[Mo(\eta^3\text{-}C_3H_5)Cl(\eta^6\text{-}C_6H_5CH_3)\{Ph_2PNHC(O)CH_3\}]$ **1** (Scheme 1) as a purple solid, in moderate yield. The characterising data for **1**, and all other new compounds **2**–**4** described in this paper, are given in Table 1.

The $^{31}P\text{-}\{^1H\}$ NMR spectrum of **1** shows a peak at δ 78.1 ppm which corresponds to a downfield shift of 57 ppm relative to the free ligand (δ 21.6 ppm in $CDCl_3$)[10] and this is consistent with coordination of the phosphorus atom to the Mo(II) centre.[14] The IR spectrum confirmed that the carbonyl fragment was not coordinated to the metal centre (ν_{co} 1698 cm^{-1} *vs.* 1715 cm^{-1} for the free ligand in CH_2Cl_2).[10]

However, the reaction between L^1 and the dinuclear complex $[Mo(\eta^3\text{-}C_3H_5)(\mu\text{-}Cl)(\eta^6\text{-}C_6H_6)]_2$ in ethanol yielded a dark red solution. The $^{31}P\text{-}\{^1H\}$ NMR spectrum of the mixture showed a signal at δ 119.4 ppm, which corresponds to a downfield shift of *ca.* 40 ppm compared to the ^{31}P chemical shift of **1**. Furthermore, in the IR spectrum the ν_{co} vibration occurred at 1602 cm^{-1}. These data suggest a chelating coordination mode of the P,O ligand, as already observed in Pd complexes,[10] and formation of the cationic complexes $[Mo(\eta^3\text{-}C_3H_5)\{Ph_2PNHC(O)CH_3\text{-}\kappa^2P,O\}(\eta^6\text{-}C_6H_6)]Cl$. Indeed, after the reaction mixture was treated with an excess of ammonium hexafluorophosphate, orange–red crystals of $[Mo(\eta^3\text{-}C_3H_5)\{Ph_2PNHC(O)CH_3\text{-}\kappa^2P,O\}(\eta^6\text{-}C_6H_6)][PF_6]$ **2a** were obtained in 33% yield (Scheme 1). The toluene analogue of **2a** $[Mo(\eta^3\text{-}C_3H_5)\{Ph_2PNHC(O)CH_3\text{-}\kappa^2P,O\}(\eta^6\text{-}C_6H_5CH_3)][PF_6]$ **2b**, was also obtained as orange–red crystals (31% yield) in a similar manner from L^1 and $[Mo(\eta^3\text{-}C_3H_5)(\mu\text{-}Cl)(\eta^6\text{-}C_6H_5CH_3)]_2$ (Scheme 1). Complexes **2a**,**b** both crystallised with one equivalent of ethanol in the crystal lattice.

The ^1H NMR spectra of **2a**,**b** showed a resonance assignable to the NH proton and this is significantly shifted to low field (**2a** δ 10.46 ppm, **2b** δ 11.60 ppm, free ligand δ 6.15 ppm in $CDCl_3$).[10] The observed shift is consistent with the amide proton undergoing hydrogen bonding with an ethanol molecule. The presence of hydrogen bonding between the NH and the OH of the ethanol solvent was confirmed from the crystal structure of **2a**·C_2H_5OH.

X-Ray quality crystals of **2a** were grown *via* the slow cooling of a hot ethanol solution of the cationic complex. The molecular structure of **2a**·C_2H_5OH is given in Figs 1 and 2. Selected bond distances and angles are listed in Table 2.

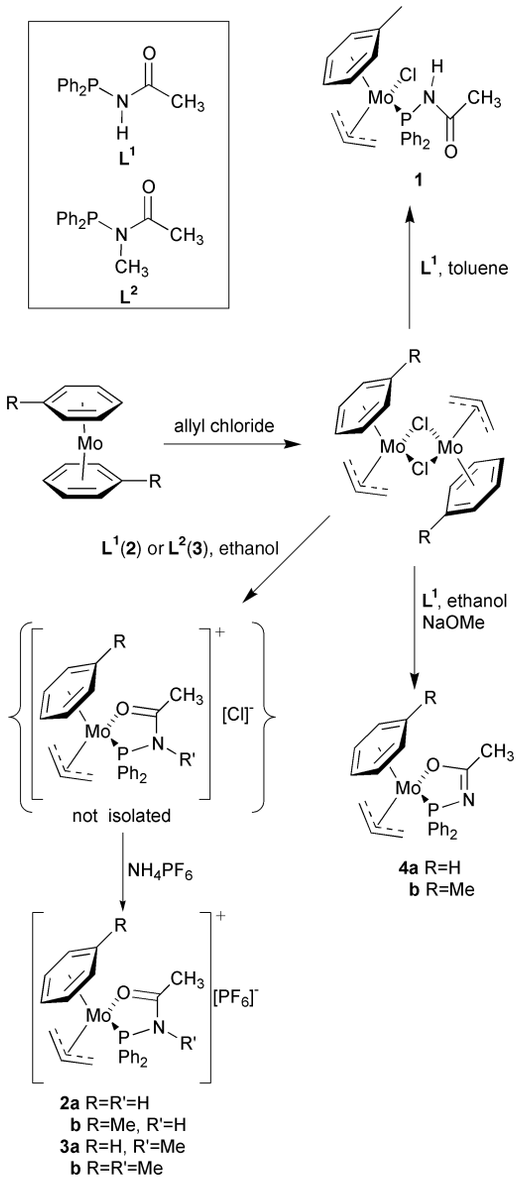

Scheme 1

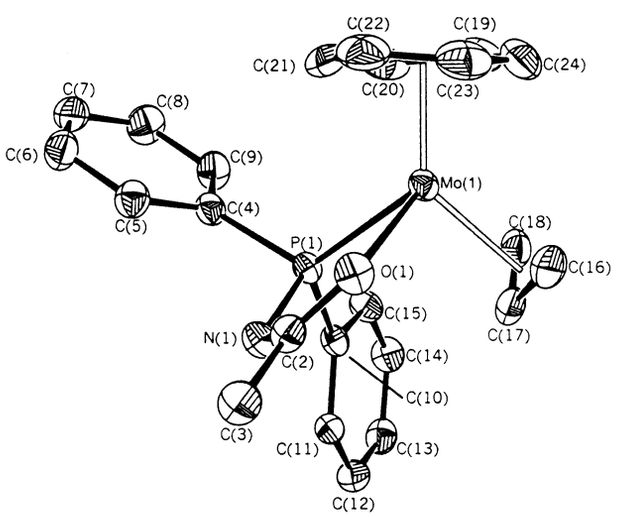

Fig. 1 Molecular structure of the cation in $[Mo(\eta^3\text{-}C_3H_5)(\eta^6\text{-}C_6H_6)\{Ph_2PNHC(O)CH_3\text{-}\kappa^2P,O\}][PF_6]\cdot C_2H_5OH$ **2a**·C_2H_5OH. (50% thermal ellipsoids). Hydrogen atoms and ethanol have been omitted for clarity.

The cationic compound **2a** adopts a three-legged piano stool structure, with the Mo-allyl centroid vector taken as one of the legs of the stool. The two enantiomers resulting from the metal-centred chirality are present in the unit cell. The average L–M–L angle of 89.2° and the average arene centroid–Mo–L angle of 124.5°, are similar to those observed in other molybdenum three-legged piano stool structures.[16,17] The Mo-ligand bond lengths and angles are within the expected ranges.[17–20]

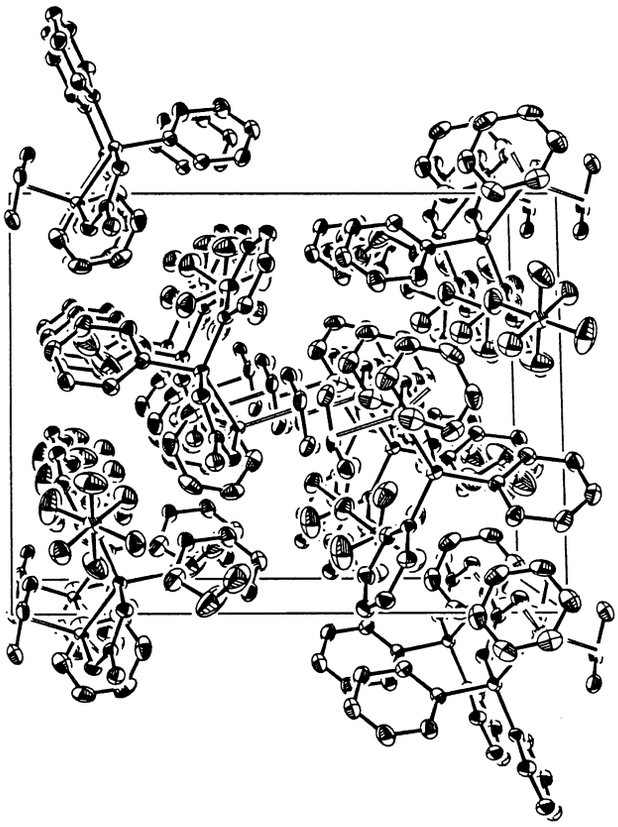

Fig. 2 Packing diagram of $[Mo(\eta^3\text{-}C_3H_5)(\eta^6\text{-}C_6H_6)\{Ph_2PNHC(O)CH_3\text{-}\kappa^2P,O\}][PF_6]\cdot C_2H_5OH$ **2a**·C_2H_5OH (50% thermal ellipsoids), viewed along the 100 axis. Hydrogen atoms have been omitted for clarity.

The structural features of the acetamide-based P,O ligand are similar to those observed in the crystal structure of the square planar cationic palladium(II) complex $[Pd(CH_3)\{PPh_2NHC(O)CH_3\text{-}\kappa^2P,O\}\{PPh_2NHC(O)CH_3\}][O_3SCF_3]$.[10]

However, the bite angle of the ligand L^1 is slightly smaller in the Mo(II) complex (75.39(4)°) compared with that in the square planar Pd(II) complex (80.5(1)°). Yet it is similar to the PCCO bite angles of 74.76(4) and 74.37(9)° observed in $[MoCpCl_3\{Ph_2PCH_2C(O)NPh_2\text{-}\kappa^2P,O\}]$ and $[MoCp^*Cl_3\{Ph_2PCH_2C(O)NPh_2\text{-}\kappa^2P,O\}][BF_4]$, respectively.[10]

The cations of **2a** form channels which lie approximately along the *x* axis and the hexafluorophosphate anions are interspersed between the C(10)–C(15) phenyl rings of the PPh_2 groups on adjacent molecules. The ethanol molecules occupy the spaces between adjacent C(4)–C(9) phenyl groups of the PPh_2 fragment (Fig. 2).

The hydrogen bonding between the ethanol oxygen and the amide proton is confirmed from the crystal structure, with an O ··· N distance of 2.82 Å. The O–H–N angle of approximately 164° is also consistent with a hydrogen bond. Similar hydrogen bonding between the amide proton and ethanol solvate molecules was observed in the crystal structure of $[NiCl(EtOH)L_2]Cl[NiCl_2L_2]$ (L = $\{Ph_2PN(H)C(O)Ph\}$).[11] A hydrogen bonding interaction between the amide proton and the amide oxygen of an adjacent molecule was also observed in the crystal structure of the free ligand $Ph_2PNHC(O)CH_3$ (N ··· O 2.83 Å, N–H–O 173.7°).[10]

The η^6-benzene ligand of **2a** adopts an inverted boat conformation.[20–23] Two carbon atoms [C(19) and C(22)] are pushed away from the metal centre, resulting in a dihedral fold angle (θ) of 9.8° at the C(19)–C(22) vector. The observed

Table 1 Analytical and spectroscopic data

Compound and analytical data [a]		NMR [b] and IR [c] data
1	$[Mo(\eta^3\text{-}C_3H_5)Cl\{Ph_2PNHC(O)CH_3\}(\eta^6\text{-}C_6H_5CH_3)]$ Purple solid C 56.3 (56.8), H 5.3 (5.4), N 2.8 (2.8)	^{1}H [d]: 8.37 (d, J_{HP} = 18, 1H, N*H*), 7.87–7.08 (m, 10H, *Ph*$_2$P), 4.35 (m, 1H, *Tol*), 4.29 (m, 1H, *Tol*), 4.26 (m, 1H, allyl H_c), 3.79 (m, 2H, *Tol*), 3.67 (t, J_{HH} = 5.7, 1H, *Tol*), 3.09 (dd, J_{HH} = 3, J_{HH} = 6, 1H, allyl H_t), 2.81 (dd, J_{HH} = 3, J_{HH} = 8, 1H, allyl H_t), 1.73 (s, 3H, C(O)C*H*$_3$), 1.68 (m, 1H, allyl H_t), 1.46 (s, 3H, tolC*H*$_3$), 1.01 (t, J_{HH} = 7.7, 1H, allyl H_t). ^{13}C-{^{1}H} [d]: 170.6 (d, J_{PC} = 12.7, N*C*(O)CH$_3$), 136.0 (d, J_{PC} = 43.7, Ph), 131.9 (d, J_{PC} = 10.9, Ph), 131.5 (unknown–under 131.9 peak), 129.9 (d, J_{PC} = 14.5, Ph), Ph resonances obscured by solvent, 115.3 (s, tol), 100.3 (s, tol), 97.0 (s, tol), 94.4 (s, tol), 93.2 (s, tol), 92.5 (s, tol), 81.8 (s, allyl C_c), 52.9 (s, allyl C_t), 43.5 (d, J_{PC} = 6, C(O)*C*H$_3$), 24.3 (s, allyl C_t), 19.0 (s, tol*C*H$_3$). ^{31}P-{^{1}H} [d]: 78.1 (s, –P*Ph*$_2$). IR: 1698 (s, ν_{co}).
2a	$[Mo(\eta^3\text{-}C_3H_5)\{Ph_2PNHC(O)CH_3\text{-}\kappa^2P,O\}(\eta^6\text{-}C_6H_6)][PF_6]$ Red crystals C 45.6 (46.2), H 4.5 (4.8), N 2.2 (2.2)	^{1}H [e]: 10.46 (br, 1H, N*H*), 8.01–7.97 (m, 2H, Ph), 7.84–7.77 (m, 2H, Ph), 7.70–7.58 (m, 6H, Ph), 5.10 (d, J_{HP} = 1.2, 6H, C$_6$*H*$_6$), 3.57 (m, 2H, HOC*H*$_2$CH$_3$), 3.47–3.32 (m, 2H, allyl H_c and H_t), 2.49 (d, J_{HP} = 0.7, 3H, C(O)C*H*$_3$), 2.02 (m, 1H, allyl H_t), 1.76 (m, 1H, allyl H_t), 1.13 (t, J_{HH} = 7.0, 3H, HOCH$_2$C*H*$_3$), 1.11 (m, 1H, allyl H_t). ^{13}C-{^{1}H} [e]: 210.0 (s, N*C*(O)CH$_3$), 135.7 (d, J_{PC} = 43.5, Ph), 131.9 (s, Ph), 131.8 (s, Ph), 131.65 (d, J_{PC} = 11.2, Ph), 130.6 (d, J_{PC} = 11.2, Ph), 129.9 (d, J_{PC} = 9.9, Ph), 129.6 (d, J_{PC} = 9.9, Ph), 129.0 (apparent s, Ph), 99.4 (s, *C*$_6$H$_6$), 79.8 (s, allyl C_c), 48.7 (s, allyl C_t), 42.5 (s, C(O)*C*H$_3$), 22.3 (s, allyl C_t). ^{31}P-{^{1}H} [e]: 119.4 (s, Ph$_2$*P*N), −143.2 (sept, J_{PF} = 708, *P*F$_6$). IR: 1602 (s, ν_{co}).
2b	$[Mo(\eta^3\text{-}C_3H_5)\{Ph_2PNHC(O)CH_3\text{-}\kappa^2P,O\}(\eta^6\text{-}C_6H_5CH_3)][PF_6]$ Red crystals C 47.2 (47.1), H 4.8 (5.0), N 2.1 (2.1)	^{1}H [g]: 11.60 (br d, J_{HP} = 3.4, 1H, N*H*), 7.89 (m, 2H, Ph), 7.76–7.61 (m, 10H, Ph), 5.30–5.22 (m, 2H, tol), 4.77 (t, J_{HH} = 5.6, 1H, tol), 4.67 (d, J_{HH} = 4.4, 1H, tol), 4.61 (t, J_{HH} = 6.0, 1H, tol), 3.22 (m, 1H, allyl H_c), 2.99 (m, 1H, allyl H_t), 2.37 (s, 3H, amide C*H*$_3$), 1.90 (m, 1H, allyl H_t), 1.56 (s, 3H, tol-C*H*$_3$), 1.54 (m, 1H, allyl H_t), 0.84 (m, 1H, allyl H_t). ^{13}C-{^{1}H} [g]: 186.8 (s, *C*O), 134.9 (d, J_{CP} = 42.7, P*Ph*$_2$), 131.0 (s, P*Ph*$_2$), 130.9 (s, P*Ph*$_2$), 130.8 (s, P*Ph*$_2$), 129.8 (s, P*Ph*$_2$), 129.1 (d, J_{CP} = 9.3, P*Ph*$_2$), 128.8 (d, J_{CP} = 10.2, P*Ph*$_2$), 119.4 (s, *Tol*), 102.7 (s, *Tol*), 98.3 (s, *Tol*), 97.4 (s, *Tol*), 96.6 (s, *Tol*), 93.3 (s, *Tol*), 91.4 (s, allyl C_c), 77.6 (s, allyl C_t), 41.4 (s, C(O)*C*H$_3$), 22.1 (s, allyl C_t), 18.9 (s, tol*C*H$_3$). ^{31}P-{^{1}H} [g]: 118.5 (s, Ph$_2$*P*N), −143.1 (sept, J_{PF} = 713, *P*F$_6$). IR: 1602 (s, ν_{co}).
3a	$[Mo(\eta^3\text{-}C_3H_5)\{Ph_2PN(CH_3)C(O)CH_3\text{-}\kappa^2P,O\}(\eta^6\text{-}C_6H_6)][PF_6]$ Orange–Red crystals C 46.7 (46.7), H 4.4 (4.4), N 2.3 (2.3)	^{1}H [e]: 7.92–7.85 (m, 4H, *Ph*$_2$PN), 7.74–7.67 (m, 6H, *Ph*$_2$PN), 5.06 (d, J_{HH} = 1, 6H, C$_6$*H*$_6$), 3.56 (m, 1H, allyl H_c), 3.26 (dd, J = 8.4, J = 2.6, 1H, allyl H_t), 3.22 (d, J_{HP} = 4, 3H, NC*H*$_3$, 2.46 (s, 3H, COC*H*$_3$), 1.98 (dd, J_{HH} = 3, J_{HH} = 6.5, 1H, allyl H_t), 1.50 (m, 1H, allyl H_t), 1.06 (m, 1H, allyl H_t). ^{13}C-{^{1}H} [e]: 189.3 (d, J_{PC} = 18, N*C*(O)CH$_3$), 133.3 (d, J_{PC} = 41, Ph), 132.5 (d, J_{PC} = 10, Ph), 132.1 (d, J_{PC} = 8, Ph), 131.7 (s, Ph), 131.6 (s, Ph), 130.1 (d, J_{PC} = 10, Ph), 129.8 (d, J_{PC} = 9.5, Ph), 125.9 (d, J_{PC} = 37.6, Ph), 80.0 (s, allyl), 48.8 (s allyl), 42.9 (d, J_{PC} = 4.2, C(O)*C*H$_3$), 37.3 (d, J_{PC} = 4.3, N*C*H$_3$), 22.7 (s, allyl). ^{31}P-{^{1}H} [e]: 150.5 (s, Ph$_2$*P*N), −143.1 (sept, J_{FP} = 708, *P*F$_6$). IR: 1580, 1570 (s, ν_{co}).
3b	$[Mo(\eta^3\text{-}C_3H_5)\{Ph_2PN(CH_3)C(O)CH_3\text{-}\kappa^2P,O\}(\eta^6\text{-}C_6H_5CH_3)][PF_6]$ Orange–Red crystals C 47.5 (47.6), H 4.6 (4.6), N 2.2 (2.2)	^{1}H [e]: 7.94–7.82 (m, 4H, *Ph*$_2$PN), 7.75–7.66 (m, 6H, *Ph*$_2$PN), 5.34 (d, J_{HH} = 5.3, 1H, tol), 5.09 (m, 1H, tol), 4.77 (d, J_{HH} = 5.3, 1H, tol), 4.69 (m, 1H, tol), 4.59 (t, J_{HH} = 6.2, 1H, tol), 3.58 (m, 1H, allyl H_c), 3.25 (d, J_{HP} = 3.8, 3H, NC*H*$_3$), 3.05 (dd, J_{HH} = 2.7, J_{HH} = 8.5, 1H, allyl H_t), 2.51 (s, 3H, C(O)C*H*$_3$), 2.02 (dd, J_{HH} = 3.3, J_{HH} = 6.4, 1H, allyl H_t), 1.67 (s, 3H, tolC*H*$_3$), 1.49 (m, 1H, allyl H_t), 0.91 (t, J_{HH} = 7.1, allyl H_t). ^{13}C-{^{1}H} [e]: 188.3 (d, J_{CP} = 17.7, *C*O), 132.4 (d, J_{CP} = 40.2, P*Ph*$_2$), 131.7 (s, P*Ph*$_2$), 131.6 (s, P*Ph*$_2$), 131.2 (d, J_{CP} = 12.1, P*Ph*$_2$), 130.6 (d, J_{CP} = 11.4, P*Ph*$_2$), 129.3 (d, J_{CP} = 9.4, P*Ph*$_2$), 129.0 (d, J_{CP} = 8.7, P*Ph*$_2$). 125.1 (d, J_{CP} = 37.5, P*Ph*$_2$), 119.7 (s, *Tol*), 102.9 (s, *Tol*). ^{31}P-{^{1}H} [e]: 151.0 (s, Ph$_2$*P*N), −143.1 (sept, J_{FP} = 708, *P*F$_6$). IR: 1580, 1568 (s, ν_{co}).
4a	$[Mo(\eta^3\text{-}C_3H_5)(\eta^6\text{-}C_6H_6)\{Ph_2PN{=}C({=}O)CH_3\text{-}\kappa^2P,O\}]$ Orange crystals	^{1}H [f]: 7.96 (m, 3H, Ph), 7.83 (m, 3H, Ph), 7.18–7.02 (m, 4H, Ph), 4.14 (s, 6H, C$_6$*H*$_6$), 3.49 (m, 1H, allyl H_c), 2.86 (dd, J_{HH} = 2.6, J_{HH} = 7.8, 1H, allyl H_t), 2.33 (s, 3H, C(O)C*H*$_3$), 2.26 (m, 1H, allyl H_t), 1.83 (m, 1H, allyl H_t), 0.48 (m, 1H, allyl H_t). ^{13}C-{^{1}H} [f]: 186.8 (d, J_{CP} = 8, *C*=N), 130.7 (d, J_{CP} = 8.6, P*Ph*$_2$), 129.6 (d, J_{CP} = 10.4, P*Ph*$_2$), 128.6 (d, J_{CP} = 1.7, P*Ph*$_2$), 128.5 (d, J_{CP} = 1.8, P*Ph*$_2$), 127.7 (d, J_{CP} = 8.7, P*Ph*$_2$), 127.3 (d, J_{CP} = 9.2, P*Ph*$_2$), 95.8 (s, C$_6$H$_6$), 76.8 (s, allyl C_c), 46.6 (s, allyl C_t), 40.3 (d, J_{CP} = 5.4, C(O)*C*H$_3$), 22.7 (d, J_{CP} = 12.4, allyl C_t). ^{31}P-{^{1}H} [f]: 107.6 (s, Ph$_2$*P*N) IR: 1506 (w, ν_{CN} + ν_{CO}).
4b	$[Mo(\eta^3\text{-}C_3H_5)(\eta^6\text{-}C_6H_6)\{Ph_2PN{=}C({=}O)CH_3\text{-}\kappa^2P,O\}]$ Orange crystals C 61.4 (61.2), H 5.8 (5.6), N 2.9 (3.0)	^{1}H [f]: 7.84–7.78 (m, 2H, *Ph*$_2$PN), 7.66–7.60 (m, 2H, *Ph*$_2$PN), 7.46–7.34 (m, 6H, *Ph*$_2$PN), 4.85–4.79 (m, 2H, tol), 4.22 (m, 1H, tol), 4.17–4.10 (m, 2H, tol), 2.92 (m, 1H, allyl H_c), 2.48 (dd, J_{HH} = 2.5, J_{HH} = 8, 1H, allyl H_t), 2.12 (d, J_{HP} = 1, 3H, COC*H*$_3$), 1.73 (m, 1H, allyl H_t), 1.52 (m, 1H, allyl H_t), 1.44 (s, 3H, tolC*H*$_3$), 0.30 (m, 1H, allyl H_t). ^{13}C-{^{1}H} [f]: 186.4 (s, *C*=N), 140.9 (d, J_{PC} = 43, *Ph*$_2$PN), 134.6 (d, J_{PC} = 40, *Ph*$_2$PN), 130.7 (d, J_{PC} = 9.7, *Ph*$_2$PN), 129.5 (d, J_{PC} = 9.7, *Ph*$_2$PN), 128.5 (d, J_{PC} = 2, *Ph*$_2$PN), 128.4 (d, J_{PC} = 2.6, *Ph*$_2$PN), 127.7 (d, J_{PC} = 8.5, *Ph*$_2$PN), 127.3 (d, J_{PC} = 9.6, *Ph*$_2$PN), 119.1 (s, tol), 102.0 (s, tol), 95.8 (s, tol), 94.9 (d, J_{PC} = 3, tol), 88.6 (d, J_{PC} = 2.4, tol), 86.6 (s, tol), 75.8 (s, allyl C_c), 46.8 (s, CO*C*H$_3$), 40.2 (d, J_{PC} = 5.2, allyl C_t), 23.2 (d, J_{PC} = 13.3, allyl C_t), 18.5 (s, tol*C*H$_3$). ^{31}P-{^{1}H} [f]: 107.6 (s, Ph$_2$*P*N) IR: 1506 (w, ν_{CN} + ν_{CO})

[a] Calculated values given in parentheses. [b] NMR data are given as chemical shift (δ) (multiplicity, relative intensity, *J*/Hz, assignment). [c] Nujol mull. [d] Recorded in C_6D_6. [e] Recorded in d_6-acetone. [f] Recorded in CD_2Cl_2. [g] Recorded in d_6-dmso.

fold angle is consistent with other observed distortions in molybdenum arene complexes. For example, the complexes $[Mo(\mu\text{-}SCH_3)_2(\eta^6\text{-}C_6H_5CH_3)]_2[PF_6]_2$ [23] and $[Mo(CH_3)_2\{PPh(CH_3)_2\}_2(\eta^6\text{-}C_6H_5CH_3)]$ [20] displayed inverted boat distortion of the arene ligand with fold angles 9.6 and 10.9°,[22] respectively. The distortion of the arene ligand is also reflected in the

Table 2 Selected bond lengths (Å) and angles (°) for **2a**·C_2H_5OH

Mo(1)–C(16)	2.255(2)	Mo(1)–C(19)	2.359(2)
Mo(1)–C(17)	2.194(2)	Mo(1)–C(20)	2.256(2)
Mo(1)–C(18)	2.257(2)	Mo(1)–C(21)	2.292(2)
Mo(1)–$Cent_{(allyl)}$	1.980	Mo(1)–C(22)	2.366(2)
Mo(1)–$C_{(average)}$	2.234	Mo(1)–C(23)	2.275(2)
		Mo(1)–C(24)	2.295(2)
Mo(1)–P(1)	2.4316(5)	Mo(1)–$Cent_{(bz)}$	1.827
Mo(1)–O(1)	2.1930(15)	Mo(1)–$C_{(average)}$	2.307
$Cent_{(bz)}$–Mo(1)–$Cent_{(allyl)}$	131.26	$Cent_{(allyl)}$–Mo(1)–O(1)	94.47
$Cent_{(bz)}$–Mo(1)–O(1)	120.01	$Cent_{(allyl)}$–Mo(1)–P(1)	97.71
$Cent_{(bz)}$–Mo(1)–P(1)	122.32	O(1)–Mo(1)–P(1)	75.39(4)
P(1)–N(1)	1.7160(17)	P(1)–N(1)–C(2)	118.07(15)
N(1)–C(2)	1.340(3)	N(1)–C(2)–O(1)	121.36(19)
C(2)–O(1)	1.250(3)		

carbon–carbon bond distances, with two bonds [C(20)–C(21) = 1.433(4), C(23)–C(24) = 1.437(4) Å] longer than the others [average = 1.40(4) Å].

The reaction between *N*-(diphenylphosphino)-*N*-methylacetamide L^2 and the dinuclear complexes $[Mo(\eta^3\text{-}C_3H_5)(\mu\text{-}Cl)(\eta^6\text{-}C_6H_5R)]_2$ (R = H, CH_3) in ethanol also yielded a dark red solution from which orange–red crystals of $[Mo(\eta^3\text{-}C_3H_5)\{Ph_2PN(CH_3)C(O)CH_3\text{-}\kappa^2P,O\}(\eta^6\text{-}C_6H_5R)][PF_6]$ **3a** (R = H), **3b** (R = CH_3) were obtained in 42–64% yields after addition of an excess of ammonium hexafluorophosphate (Scheme 1).

The $^{31}P\text{-}\{^1H\}$ NMR and IR spectra of **3a**,**b** were consistent with the P,O ligand coordinating as a bidentate ligand to form a cationic Mo(II) complex (Table 1).

X-Ray quality crystals of **3a** were grown *via* the slow cooling of a hot ethanol solution of the cationic complex. The crystal structure of the complex **3a** has been determined and the molecular structure is shown in Fig 3. Selected bond distances and angles are presented in Table 3.

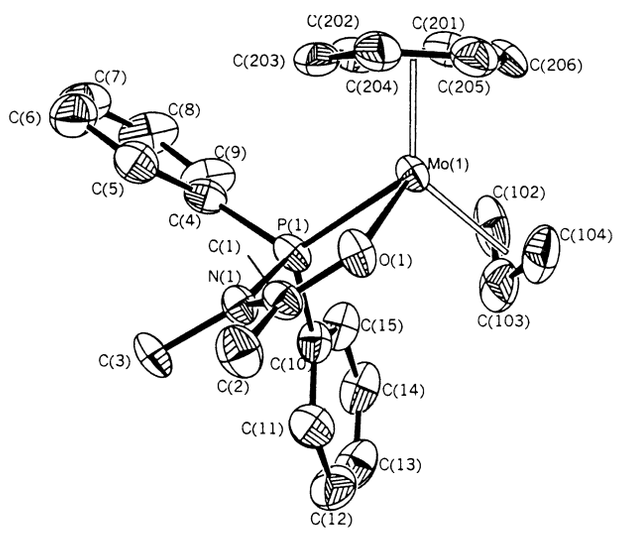

Fig. 3 Molecular structure of the cation in $[Mo(\eta^3\text{-}C_3H_5)\{Ph_2PN(CH_3)C(O)CH_3\text{-}\kappa^2P,O\}(\eta^6\text{-}C_6H_6)][PF_6]$ **3a** (50% thermal ellipsoids). Hydrogen atoms have been omitted for clarity. The benzene and allyl groups are disordered over common sites (see text).

The cationic complex adopts a three-legged piano stool structure, as observed for the crystal structure of **2a**. Similarly, the two enantiomers, resulting from the metal-centred chirality are present in the unit cell. The Mo–ligand bond lengths and angles are within expected ranges.[17–20]

As for the complex **2a**, the molecules pack in such a way to generate chains along the *x* axis (100) of the crystal. The hexafluorophosphate anions occupy spaces between the allyl ligands of adjacent molecules along the chain.

The crystal structure of **3a** displayed some disorder of the arene and allyl ligands. Since the complex is chiral at the molybdenum centre, exchanging the positions of the benzene and allyl ligands produces the other enantiomer (enantiomers A and B). However, the molecule exists in its racemic form and crystallises in an achiral space group. The observed disorder is due to distortion in the crystal packing, with 40% of enantiomer A occupying sites otherwise occupied by enantiomer B and *vice versa*.

The reaction between L^1, $[Mo(\eta^3\text{-}C_3H_5)(\mu\text{-}Cl)(\eta^6\text{-}C_6H_5R)]_2$ (R = H, CH_3) and an excess of sodium methoxide in ethanol yielded a dark red solution from which orange crystals of $[Mo(\eta^3\text{-}C_3H_5)(\eta^6\text{-}C_6H_5R)\{Ph_2PN{=}C(^-O)CH_3\text{-}\kappa^2P,O\}]$ **4a** (R = H), **4b** (R = CH_3) were isolated in 75 and 30% yield for **4a** and **4b**, respectively (Scheme 1).

A $^{31}P\text{-}\{^1H\}$ NMR resonance at δ 107.6 ppm was observed for both complexes. The IR spectra of **4a**,**b** exhibited a band at 1506 cm^{-1} which was ascribed to a $\nu_{CN} + \nu_{CO}$ vibration. These data are consistent with the formation of an η^2-phosphinoiminolate complex (Table 1).

X-Ray quality crystals of **4a** were grown from a concentrated dichloromethane–pentane solution at −20 °C. The molecular structure of complex **4a** is given in Fig. 4. Selected bond

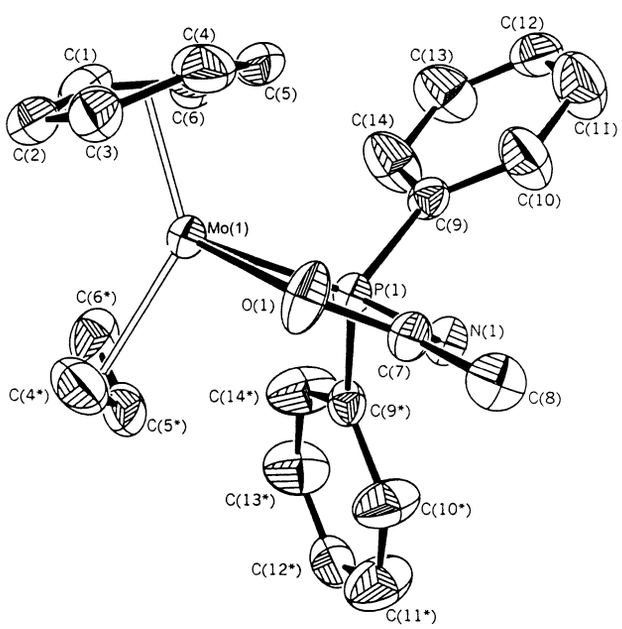

Fig. 4 Molecular structure of $[Mo(\eta^3\text{-}C_3H_5)(\eta^6\text{-}C_6H_6)\{PhP_2N{=}C(^-O)CH_3\text{-}\kappa^2P,O\}]$ **4a** (50% thermal ellipsoids). Hydrogen atoms have been omitted for clarity. The benzene and allyl groups are disordered over two sites equivalent by symmetry (see text).

distances and angles are presented in Table 4. The neutral complex **4a** adopts a three-legged piano stool structure, as observed for the crystal structures of **2a** and **3a** and likewise, the

Table 3 Selected bond lengths (Å) and angles (°) for **3a**

Mo(1)–C(102)	2.263(6)	Mo(1)–C(201)	2.314(8)
Mo(1)–C(103)	2.225(6)	Mo(1)–C(202)	2.247(6)
Mo(1)–C(104)	2.293(6)	Mo(1)–C(203)	2.238(5)
Mo(1)–$Cent_{(allyl)}$	2.014	Mo(1)–C(204)	2.320(5)
Mo(1)–$C_{(average)}$	2.264	Mo(1)–C(205)	2.289(8)
		Mo(1)–C(206)	2.253(8)
Mo(1)–P(1)	2.4123(12)	Mo(1)–$Cent_{(bz)}$	1.782
Mo(1)–O(1)	2.161(3)	Mo(1)–$C_{(average)}$	2.280
$Cent_{(bz)}$–Mo(1)–$Cent_{(allyl)}$	129.06	$Cent_{(allyl)}$–Mo(1)–O(1)	99.48
$Cent_{(bz)}$–Mo(1)–O(1)	116.42	$Cent_{(allyl)}$–Mo(1)–P(1)	99.17
$Cent_{(bz)}$–Mo(1)–P(1)	123.24	O(1)–Mo(1)–P(1)	75.29(9)
P(1)–N(1)	1.735(4)	P(1)–N(1)–C(1)	116.4(3)
N(1)–C(1)	1.347(6)	N(1)–C(1)–O(1)	120.7(4)
C(1)–O(1)	1.251(6)	N(1)–C(3)	1.482(6)

Table 4 Selected bond lengths (Å) and angles (°) for **4a**

Mo(1)–C(4*)	2.302(5)	Mo(1)–C(1)	2.383(7)
Mo(1)–C(5*)	2.231(4)	Mo(1)–C(2)	2.294(7)
Mo(1)–C(6*)	2.248(4)	Mo(1)–C(3)	2.292(7)
Mo(1)–$Cent_{(allyl)}$	2.007	Mo(1)–C(4)	2.302(5)
Mo(1)–$C_{(average)}$	2.26	Mo(1)–C(5)	2.231(4)
		Mo(1)–C(6)	2.248(4)
Mo(1)–P(1)	2.4471(14)	Mo(1)–$Cent_{(bz)}$	1.825
Mo(1)–O(1)	2.152(4)	Mo(1)–$C_{(average)}$	2.29
$Cent_{(bz)}$–Mo(1)–$Cent_{(allyl)}$	132.88	$Cent_{(allyl)}$–Mo(1)–O(1)	99.35
$Cent_{(bz)}$–Mo(1)–O(1)	112.73	$Cent_{(allyl)}$–Mo(1)–P(1)	97.76
$Cent_{(bz)}$–Mo(1)–P(1)	123.23	O(1)–Mo(1)–P(1)	73.8(1)
P(1)–N(1)	1.679(4)	P(1)–N(1)–C(7)	113.6(3)
N(1)–C(7)	1.298(7)	N(1)–C(7)–O(1)	125.9(5)
C(7)–O(1)	1.291(6)	C(7)–C(8)	1.508(7)

enantiomers, resulting from the metal-centred chirality, are present in the unit cell. The Mo-ligand bond lengths and angles are within expected ranges. This is the first example of a structurally characterised η^2-phosphinoiminolate complex. The metallacyclic fragment, Mo(1)–P(1)–N(1)–C(7)–O(1), is planar and the methyl carbon [C(8)] is also lying in this plane.

Deprotonation of the phosphino–acetamide complex **2a** to give the corresponding phosphinoiminolate complex **4a** has little effect upon the Mo–P bond length [2.4471(14) Å *vs.* 2.4316(5) and 2.4123(12) Å for **2a** and **3a**, respectively] or the P–Mo–O bite angle of the chelating ligand [73.8(1) *vs.* 75.39(4) and 75.29(9)° for **2a** and **3a**, respectively]. However a shortening of the Mo–O [2.152(4)], P–N [1.679(4)] and N–C [1.298(7) Å] bonds and a lengthening of the C–O [1.291(6) Å] bond is observed. These observed changes are consistent with the formation of a phosphinoiminolate ligand.

Because the molecule lies on a mirror plane defined by Mo(1)–P(1)–N(1)–C(7)–O(1), the allyl and arene groups are inevitably 50% disordered over the two equivalent sites. The atoms of the allyl group essentially overlap (in the disorder) three of the arene carbons, so that these appear at full occupancy in the list of atomic coordinates.

Conclusion

A series of arene molybdenum complexes in which the amide-derived ligands $Ph_2PN(R)C(O)CH_3$ (R = H, CH_3) display η^1-phosphine, η^2-acetamidophosphine and η^2-phosphinoiminolate coordination have been synthesised and characterised. The X-ray crystal structure determination of the phosphinoiminolate complex $[Mo(\eta^3\text{-}C_3H_5)(\eta^6\text{-}C_6H_6)\{PhP_2N{=}C({=}O)CH_3\text{-}\kappa^2P,O\}]$ represents the first structurally characterised example of this class of chelating ligand. The crystal structures of the cationic compounds $[Mo(\eta^3\text{-}C_3H_5)(\eta^6\text{-}C_6H_6)\{Ph_2PN(R)C(O)CH_3\text{-}\kappa^2P,O\}][PF_6]$ (R = H, CH_3) have also been determined.

The results described here present the first investigations into the chemistry of acetamide derived ligands with a middle transition metal species.

Experimental

General

All manipulations of air- and/or moisture sensitive materials were performed under an inert atmosphere of argon using standard Schlenk line techniques, or in an inert atmosphere dry box containing dinitrogen. Solvents were dried over the appropriate drying agent and distilled under nitrogen. Deuterated solvents were dried over the appropriate drying agent and vacuum distilled prior to use.

The compounds $[Mo(\eta^3\text{-}C_3H_5)(\mu\text{-}Cl)(\eta^6\text{-}C_6H_5R)]_2$ (R = H, CH_3)[24] and $Ph_2PN(R)C(O)CH_3$ (R = H, CH_3)[10] were prepared according to previously published methods.

NMR spectra were recorded on a Varian Mercury 300 (^{1}H, ^{13}C and ^{31}P at 300.17, 75.48 and 121.51 MHz respectively) spectrometer at room temperature in d_6-acetone, d_6-dimethylsulfoxide or d_2-dichloromethane. They were referenced internally using the residual protio solvent (^{1}H) and solvent (^{13}C) resonances and measured relative to tetramethylsilane (^{1}H and ^{13}C; δ 0 ppm). ^{31}P NMR were referenced externally to 85% H_3PO_4 (δ 0 ppm). Elemental analyses were provided by the microanalytical department, Inorganic Chemistry Laboratory, University of Oxford. Infrared spectra were recorded as a mull in Nujol on a Perkin Elmer 1600 Series FTIR spectrometer.

Preparations

$[Mo(\eta^3\text{-}C_3H_5)Cl(\eta^6\text{-}C_6H_5CH_3)\{Ph_2PNHC(O)CH_3\}]$ 1. $[Mo(\eta^3\text{-}C_3H_5)(\mu\text{-}Cl)(\eta^6\text{-}C_6H_5CH_3)]_2$ (167 mg, 0.32 mmol) and $Ph_2PN(H)C(O)CH_3$ (160 mg, 0.66 mmol) were combined as solids and dissolved in toluene (20 ml). The reaction mixture

Table 5 Crystal data and structure refinement for compounds **2a**, **3a** and **4a**

	2a	**3a**	**4a**
Empirical formula	$C_{25}H_{31}F_6MoNO_2P_2$	$C_{24}H_{27}F_6MoNOP_2$	$C_{23}H_{24}MoNOP$
M	649.40	617.36	457.36
Crystal system	Monoclinic	Monoclinic	Orthorhombic
Space group	$P2_1/n$	$P2_1/c$	$Cmca$
a/Å	10.8978(2)	11.4697(5)	14.8887(8)
b/Å	18.1501(3)	13.7585(8)	16.5295(8)
c/Å	14.0945(3)	16.5254(9)	16.1773(9)
β/°	104.2295(6)	105.4(1)	90
U/Å^3	2702.3	2513.8	3981.3
Z	4	4	8
T/K	150	150	150
μ/mm^{-1}	0.67	0.71	0.75
Reflections collected	6343	5979	2362
Independent reflections	5053	3076	1511
R	0.0311	0.0417	0.0356
R_w	0.0392	0.0471	0.0387

was stirred at 65 °C for 3 h. The resulting dark red–purple solution was filtered and the filtrate reduced to small volume *in vacuo*. The product was precipitated by addition of pentane, isolated by filtration and dried *in vacuo*. Complex **1** (145 mg, 0.29 mmol, 45%) was obtained as a pale purple solid.

[Mo(η^3-C_3H_5){$Ph_2PNHC(O)CH_3$-κ^2*P*,*O*}(η^6-C_6H_6)][PF_6] 2a. [Mo(η^3-C_3H_5)(μ-Cl)(η^6-C_6H_6)]$_2$ (151 mg, 0.30 mmol) and Ph_2-PN(H)C(O)CH_3 (150 mg, 0.62 mmol) were combined as solids and suspended in ethanol (20 ml). The reaction mixture was stirred at 60–70 °C for 4 h. The resulting orange–red solution was filtered into a solution of ammonium hexafluorophosphate (200 mg) in ethanol (5 ml). The reaction was allowed to stand at room temperature for 2 h and then cooled at −20 °C for 1 h. The resulting precipitate was isolated by filtration and dried *in vacuo*. Complex **2a** (121 mg, 0.2 mmol, 33%) was obtained as an orange–red crystalline solid.

[Mo(η^3-C_3H_5){$Ph_2PNHC(O)CH_3$-κ^2*P*,*O*}(η^6-$C_6H_5CH_3$)][PF_6] 2b. This compound was prepared in a manner similar to **2a**, starting from [Mo(η^3-C_3H_5)(μ-Cl)(η^6-$C_6H_5CH_3$)]$_2$ (140 mg, 0.26 mmol) and $Ph_2PN(H)C(O)CH_3$ (130 mg, 0.53 mmol). However, the reaction was carried out at room temperature. Complex **2b** (100 mg, 0.16 mmol, 31%) was obtained as a red crystalline solid.

[Mo(η^3-C_3H_5){$Ph_2PN(CH_3)C(O)CH_3$-κ^2*P*,*O*}(η^6-C_6H_6)][PF_6] 3a. [Mo(η^3-C_3H_5)(μ-Cl)(η^6-C_6H_6)]$_2$ (105 mg, 0.21 mmol) and $Ph_2PN(CH_3)C(O)CH_3$ (120 mg, 0.47 mmol) were combined as solids and suspended in ethanol (20 ml). The reaction mixture was stirred at 60–70 °C for 4 h. The resulting orange–red solution was filtered into a solution of ammonium hexafluorophosphate (200 mg) in ethanol (5 ml). The reaction was allowed to stand at room temperature overnight. The resulting precipitate was isolated by filtration and dried *in vacuo*. Complex **3a** (167 mg, 0.27 mmol, 64%) was obtained as an orange crystalline solid.

[Mo(η^3-C_3H_5){$Ph_2PN(CH_3)C(O)CH_3$-κ^2*P*,*O*}(η^6-$C_6H_5CH_3$)]-[PF_6] 3b. This compound was prepared in a manner similar to **3a**, starting from [Mo(η^3-C_3H_5)(μ-Cl)(η^6-$C_6H_5CH_3$)]$_2$ (140 mg, 0.26 mmol) and $Ph_2PN(CH_3)C(O)CH_3$ (140 mg, 0.54 mmol). However, the reaction was carried out at room temperature. Complex **3b** (142 mg, 0.22 mmol, 42%) was obtained as a red crystalline solid.

[Mo(η^3-C_3H_5)(η^6-C_6H_6){$Ph_2PN{=}C(O)CH_3$-κ^2*P*,*O*}] 4a. [Mo-(η^3-C_3H_5)(μ-Cl)(η^6-C_6H_6)]$_2$ (100 mg, 0.20 mmol) and Ph_2PN-(H)C(O)CH_3 (105 mg, 0.43 mmol) were combined as solids and suspended in ethanol (20 ml). Excess sodium methoxide (30% solution in methanol, 3 ml) was added and the reaction mixture stirred at 65 °C for 2 h. The solvent was removed *in vacuo* and the residue extracted with dichloromethane (30 ml). The solvent was removed *in vacuo* and the resulting red–orange residue washed with cold hexane (10 ml). Complex **4a** (134 mg, 0.30 mmol, 75%) was obtained as an orange solid.

[Mo(η^3-C_3H_5)(η^6-$C_6H_5CH_3$){$Ph_2PN{=}C(O)CH_3$-κ^2*P*,*O*}] 4b. [Mo(η^3-C_3H_5)(μ-Cl)(η^6-$C_6H_5CH_3$)]$_2$ (166 mg, 0.31 mmol) and $Ph_2PN(H)C(O)CH_3$ (160 mg, 0.66 mmol) were combined as solids and suspended in ethanol (20 ml). Excess sodium methoxide (30% solution in methanol, 3 ml) was added and the reaction stirred at room temperature for 2 h. The solvent was removed *in vacuo* and the residue extracted with hexane (2 × 60 ml). The combined extracts were reduced to small volume and cooled to −20 °C overnight. The product was isolated by filtration and dried *in vacuo*. Complex **4b** (85 mg, 0.18 mmol, 30%) was obtained as an orange crystalline solid.

Crystallography

Data were collected on a Nonius KappaCCD diffractometer with Mo-Kα radiation (λ = 0.71069 Å). The images were processed with DENZO[25] and SCALEPACK[26] programs. All solution, refinement and graphical calculations were performed using CRYSTALS[27] and CAMERON[28] software packages.

In each case, a single crystal was encased in perfluoropolyether oil and mounted atop a glass fibre. The fibre, secured in a goniometer head, was placed under a stream of cold nitrogen maintained at 150 K and data collected.

The structure was solved using the program SIR92[29] and refined using full-matrix least-squares on all F data (CRYSTALS). All non-hydrogen atoms were refined anisotropically and hydrogen atoms were included in calculated positions with isotropic thermal parameters. All calculations were carried out on a Pentium personal computer.

A Chebychev polynomial weighting scheme[30] with the parameters 1.06, 0.469 and 0.735 was applied to the crystal structure of compound **2a** giving a final R factor of 0.0311 and R_w = 0.0392 with a maximum residual electron density of 0.84 e Å^{-3}. A similar weighting scheme was applied to the structure of **3a** using the parameters 0.688, 0.249 and 0.403. This yielded a final R factor of 0.0417, R_w = 0.0471 with a maximum residual electron density of 0.63 e Å^{-3}. A similar weighting scheme was applied to the structure of **4a** using the parameters 0.507, 0.0919 and 0.212. This yielded a final R factor of 0.0356, R_w = 0.0387 with a maximum residual electron density of 0.64 e Å^{-3}. The crystallographic data are given in Table 5.

CCDC reference numbers 169296–169298.

See http://www.rsc.org/suppdata/dt/b1/b105957m/ for crystallographic data in CIF or other electronic format.

Acknowledgements

We thank Dr David Watkin for assistance with the crystallography. We also wish to thank the University of Sydney, Australia and The King's School, Sydney, Australia for financial support (N. G. J), the Centre National de la Recherche Scientifique/Royal Society cooperation programme (X. M., N. G. J) and the A.G. Leventis Foundation (I. V) for financial support.

References

1 C. S. Slone, D. A. Weinberger and C. A. Mirkin, *Prog. Inorg. Chem.*, 1999, **48**, 233.
2 A. Bader and E. Lindner, *Coord. Chem. Rev.*, 1991, **108**, 27.
3 P. Braunstein and F. Naud, *Angew. Chem., Int. Ed.*, 2001, **40**, 681.
4 I. Bachert, I. Bartusseck, P. Braunstein, E. Guillon, J. Rosé and G. Kickelbick, *J. Organomet. Chem.*, 1999, **588**, 144.
5 P. Braunstein, R. Hasselbring, A. Tiripicchio and F. Ugozzoli, *J. Chem. Soc., Chem. Commun.*, 1995, 37.
6 P. Braunstein, R. Hasselbring, A. DeCian and J. Fischer, *Bull. Soc. Chim. Fr.*, 1995, **132**, 691.
7 J. T. Mague, *J. Cluster Sci.*, 1995, **6**, 217.
8 L. K. Peterson and E. W. Ainscough, *Inorg. Chem.*, 1970, **9**, 2699.
9 S. M. Aucott, A. M. Z. Slawain and J. D. Wollins, *J. Chem. Soc., Dalton Trans.*, 2000, 2559.
10 P. Braunstein, C. Frison, X. Morise and R. D. Adams, *J. Chem. Soc., Dalton Trans.*, 2000, 2205.
11 P. Bhattacharyya, T. Q. Ly, A. M. Z. Slawin and J. D. Woollins, *Polyhedron*, 2001, **20**, 1803.
12 T. Q. Ly, A. M. Z. Slawin and J. D. Woollins, *Polyhedron*, 1999, **18**, 1761.
13 P. Braunstein, C. Frison and X. Morise, *Angew. Chem., Int. Ed.*, 2000, **39**, 2867.
14 J. M. Camus, D. Morales, J. Andrieu, P. Richard, R. Poli, P. Braunstein and F. Naud, *J. Chem. Soc., Dalton Trans.*, 2000, 2577.
15 C. D. Andrews, A. D. Burrows, J. M. Lynam, M. F. Mahon and M. T. Palmer, *New J. Chem.*, 2001, **25**, 824.
16 F. Abugideiri, J. C. Fettinger, D. W. Keogh and R. Poli, *Organometallics*, 1996, **15**, 4407.
17 M. T. Ashby, V. S. Asirvatham, A. S. Kowalski and M. A. Khan, *Organometallics*, 1999, **18**, 5004.
18 C. P. Mehnert, A. N. Chernaga and M. L. H. Green, *J. Organomet. Chem.*, 1996, **513**, 247.
19 P. W. Jolly, C. Krüger, C. C. Romão and M. J. Romão, *Organometallics*, 1984, **3**, 936.
20 J. L. Atwood, W. E. Hunter, R. D. Rogers, E. Carmona-Guzman and G. Wilkinson, *J. Chem. Soc., Dalton Trans.*, 1979, 1519.
21 W. E. Silverthorn, C. Couldwell and K. Prout, *J. Chem. Soc., Chem. Commun.*, 1978, 1009.
22 P. A. Wexler, D. E. Wigley, J. B. Koerner and T. A. Albright, *Organometallics*, 1991, **10**, 2319.
23 L. J. Radonovich, F. J. Koch and T. A. Albright, *Inorg. Chem.*, 1980, **19**, 3373.
24 M. L. H. Green and W. E. Silverthorn, *J. Chem. Soc., Dalton Trans.*, 1973, 301.
25 Z. Otwinowski, in DENZO©, Department of Molecular Biophysics and Biochemistry, Yale University, New Haven, CT, US, 1993.
26 Z. Otwinowski, in SCALEPACK©, Department of Molecular Biophysics and Biochemistry, Yale University, New Haven, CT, US, 1993.
27 D. J. Watkin, C. K. Prout, J. R. Carruthers and P. W. Betteridge, in *Crystals Issue 10, Chemical Crystallography Laboratory*, University of Oxford, UK, 1996.
28 D. J. Watkin, C. K. Prout and L. J. Pearce, CAMERON, Chemical Crystallography Laboratory, University of Oxford, UK, 1996.
29 A. Altomare, G. Cascarano, C. Giacovazzo, A. Guagliardi, M. C. Burla, G. Polidori and M. Camalli, *J. Appl. Crystallogr., Sect. A*, 1994, **27**, 435.
30 R. Carruthers and D. J. Watkin, *Acta Crystallogr., Sect. A*, 1979, **35**, 698.